Development 138, 4451-4463 (2011) doi:10.1242/dev.071381

Integrin-dependent and -independent functions of astrocytic fibronectin in retinal angiogenesis

Denise Stenzel[1,*], Andrea Lundkvist[1,†], Dominique Sauvaget[1], Marta Busse[1], Mariona Graupera[2], Arjan van der Flier[3], Errol S. Wijelath[4], Jacqueline Murray[4], Michael Sobel[4], Mercedes Costell[5], Seiichiro Takahashi[6], Reinhard Fässler[6], Yu Yamaguchi[7], David H. Gutmann[8], Richard O. Hynes[3] and Holger Gerhardt[1,9,‡]

SUMMARY

Fibronectin (FN) is a major component of the extracellular matrix and functions in cell adhesion, cell spreading and cell migration. In the retina, FN is transiently expressed and assembled on astrocytes (ACs), which guide sprouting tip cells and deposit a provisional matrix for sprouting angiogenesis. The precise function of FN in retinal angiogenesis is largely unknown. Using genetic tools, we show that astrocytes are the major source of cellular FN during angiogenesis in the mouse retina. Deletion of astrocytic FN reduces radial endothelial migration during vascular plexus formation in a gene dose-dependent manner. This effect correlates with reduced VEGF receptor 2 and PI3K/AKT signalling, and can be mimicked by selectively inhibiting VEGF-A binding to FN through intraocular injection of blocking peptides. By contrast, AC-specific replacement of the integrin-binding RGD sequence with FN-RGE or endothelial deletion of *itga5* shows little effect on migration and PI3K/AKT signalling, but impairs filopodial alignment along AC processes, suggesting that FN-integrin α5β1 interaction is involved in filopodial adhesion to the astrocytic matrix. AC FN shares its VEGF-binding function and cell-surface distribution with heparan-sulfate (HS), and genetic deletion of both FN and HS together greatly enhances the migration defect, indicating a synergistic function of FN and HS in VEGF binding. We propose that in vivo the VEGF-binding properties of FN and HS promote directional tip cell migration, whereas FN integrin-binding functions to support filopodia adhesion to the astrocytic migration template.

KEY WORDS: Angiogenesis, Tip cells, Extracellular matrix, Cell migration, Endothelial guidance

INTRODUCTION

During retinal vascular development, astrocyte (AC) precursors enter the fibre layer of the inner retina through the optic nerve and radiate towards the periphery. Blood vessels subsequently follow the astrocytic network, stimulated by the hypoxia-induced expression and secretion of vascular endothelial growth factor A (VEGFA) by ACs (Stone et al., 1995). The leading endothelial tip cells that head each vascular sprout express high levels of the VEGF receptor 2 (VEGFR2) and migrate along the astrocytic network tracking the extracellular gradient of VEGFA (Ruhrberg et al., 2002; Gerhardt et al., 2003). Endothelial tip-cell filopodia closely align with the astrocytic network, suggesting controlled astrocytic-endothelial cell interaction. Fibronectin (FN) is expressed by retinal ACs in the rat retina (Jiang et al., 1994), and defective FN matrix assembly has been suggested to cause retinal vascularization defects (Uemura et al., 2006). However, the functional relevance of astrocytic FN for retinal vascular development and tip-cell guidance has not been addressed experimentally.

FN is a major component of the vascular basement membrane (BM) and mediates binding and assembly of extracellular matrix components (ECM), provides structural support for cell adhesion, triggers integrin-mediated signalling and F-actin rearrangements, and controls the availability of growth factors [summarized in Leiss et al. (Leiss et al., 2008)]. The functional relevance of FN is underscored by the dramatic consequences of genetic deletion of FN in mouse embryogenesis. FN-null embryos die at E8.5 due to severe mesodermal, vascular and neural tube defects (George et al., 1993). Detailed analysis of the cardiovascular system revealed that FN is essential for the organization of heart and blood vessels, but is dispensable for cellular specification in the appropriate regions within the embryo (George et al., 1997).

FN is secreted as a disulfide-bonded dimer that is composed of an array of three different types of domains (called FN type I, II and III domains) and assembled into a fibrillar matrix in a cell-driven process that is crucially dependent on integrin interaction. The main cell-surface receptors for FN are the heterodimeric, transmembrane glycoprotein, integrin α5β1 and the αv-containing integrins (αvβ3, αvβ5, αvβ6, αvβ8). Absence of genes encoding both integrin α5 and integrin αv in double knockout mutants compromises assembly of a FN-rich matrix and fibril formation

[1]Vascular Biology Laboratory, London Research Institute – Cancer Research UK, London WC2A 3PX, UK. [2]Grup de Angiogènesi, Laboratori d'Oncologia Molecular (LOM), Institut d'Investigació Biomèdica de Bellvitge (IDIBELL), Hospital Duran i Reynals – 3ª Planta, Gran Via de l'Hospitalet 199-203. 08907 L'Hospitalet de Llobregat, Barcelona, Spain. [3]Howard Hughes Medical Institute, Koch Institute for Integrative Cancer Research, E17-227, MIT, Cambridge, MA 02139, USA. [4]Department of Surgery, Division of Vascular Surgery, Veterans Affairs Puget Sound Health Care System and the University of Washington School of Medicine, Seattle, WA 98195, USA. [5]Departament de Bioquimica i Biologia Molecular, Universitat de València, E-46100 Burjassot, Spain. [6]Department of Molecular Medicine, Max-Planck Institute of Biochemistry, D-82152 Martinsried, Germany. [7]Sanford Children's Health Research Center, Sanford-Burnham Medical Research Institute, La Jolla, CA 92037, USA. [8]Department of Neurology, Washington University School of Medicine, St Louis, MO 63110, USA. [9]Consultant Group Leader, Vascular Patterning Laboratory, Vesalius Research Center, VIB, Campus Gasthuisberg, B-3000 Leuven, Belgium.

*Present address: Max-Planck Institute of Molecular Cell Biology and Genetics, Pfotenhauerstr. 108, 01307 Dresden, Germany
†Present address: BioInvent International AB, Sölvegatan 41, SE-223 70 Lund, Sweden
‡Author for correspondence (holger.gerhardt@cancer.org.uk)

Accepted 1 August 2011

(Yang et al., 1999). Cell adhesion to FN depends on the RGD motif (arginine-glycine-asparagine) that is located in the 10th type III domain and mediates binding to many integrins, including α5β1 and αv-containing integrins. Substitution of the integrin-binding RGD motif with an inactive RGE motif results in early embryonic lethality owing to severe defects in the posterior mesoderm (Takahashi et al., 2007). However, FN assembly is not dependent on RGD-mediated integrin binding in vivo, possibly owing to redundant activity of an integrin αvβ3-binding sequence in the 5th type I domain (Leiss et al., 2008).

FN controls the availability of growth factors, for example by regulating their activation from latent complexes, as shown for TGFβ (Fontana et al., 2005). Wijelath and colleagues mapped two binding domains on FN that modulate the activity of the angiogenic factor VEGFA. Further analysis demonstrated that VEGFA binds to a region in the 13th and 14th type III ($FnIII_{13-14}$) domain of FN, and that the cell-binding and VEGFA-binding domains of FN, when physically linked, are necessary and sufficient to promote VEGFA-induced endothelial cell (EC) proliferation, migration and extracellular signal-regulated kinase (ERK) activation (Wijelath et al., 2002; Wijelath et al., 2006).

Although FN interactions with integrin α5β1 and VEGF have been described previously, it still remains unclear whether these interactions are essential for endothelial cell adhesion, proliferation and vessel migration in vivo. To elucidate the precise role of astrocytic FN during retinal vessel formation, we specifically deleted FN from ACs using GFAP Cre mice (Bajenaru et al., 2002). Our study revealed that loss of astrocytic FN results in a surprisingly mild, but mechanistically informative, vascular defect characterized by delayed vessel extension towards the retinal periphery. We find that FN RGD motif function and endothelial expression of integrin α5 are dispensable for fibrillar FN assembly and vessel migration but contribute to endothelial tip-cell filopodial adhesion in vivo. Instead, migration appears to involve a second and α5β1-integrin-independent function of FN mediated by binding and retention of VEGFA, which in turn stimulates VEGFR2 and phosphoinositide 3-kinases (PI3K)/AKT signalling.

MATERIALS AND METHODS

Animals

Animals were housed in individually ventilated cages under barrier conditions in the animal facility of the London Research Institute (London, UK) and bred on C57Bl/6 background.

$FN^{flox/flox}$ mice (Sakai et al., 2001) were crossed to *Gfap-Cre* (Bajenaru et al., 2002), referred to as FN^{ACko}, and to *Nestin-Cre* (Petersen et al., 2002), respectively. Cre-negative and $FN^{wt/wt}$ Cre-positive littermates were used as controls.

To analyse the functional role of RGD-binding motif in astrocytic FN, FN^{ACko} were bred to heterozygous FN RGE mice (Takahashi et al., 2007).

Integrin $\alpha5^{flox/flox}$ (van der Flier et al., 2010) were crossed to integrin $\alpha5^{+/-}$ (Yang et al., 1993); Tie2-Cre (Tek-Cre) (Kisanuki et al., 2001). The Itga5 crosses were of mixed 129S4/C57BL/6J/ background and mice were housed under specific pathogen-free conditions at the Massachusetts Institute of Technology, under appropriate licences within local and national guidelines for animal care. $\alpha5^{flox/-}$ Tie-Cre mice were endothelial and hematopoeitic α5 null, controls were littermates with the following genotypes $\alpha5^{flox/-}$, $\alpha5^{flox/wt}$ and $\alpha5^{flox/wt}$ Tie-Cre.

Further $FN^{flox/flox}$ mice were crossed with *Pdgfrb* Cre (referred to as FN PCko) (Foo et al., 2006), *Pdgfb* iCreERT (referred to as FN ECko) (Claxton et al., 2008) and compound *Gfap* Cre plus *Pdgfb* iCreERT (FN AC/ECko), as well as *Pdgfrb* Cre plus *Pdgfb* iCreERT (FN EC/PCko).

$Ext1^{flox/flox}$ mice and $Ext1^{flox/flox}$ (Inatani et al., 2003) mice were crossed with *Gfap* Cre to generate mice deficient in astrocytic fibronectin and heperan sulfate (HS).

Immunofluorescence staining

Eyes were collected at postnatal (P) day 5 and fixed in 4% paraformaldehyde (PFA) for 2 hours at room temperature before transferring to phosphate-buffered saline (PBS). Retinas were dissected clean and stained as whole mounts as previously described (Gerhardt et al., 2003). Antibodies used were: isolectin-B4 (1:10, Sigma-Aldrich, Dorset, UK), directly conjugated isolectin-B4 Alexa488 and A568 (1:500, Molecular Probes Invitrogen, Paisley, UK), biotinylated PDGFRα (1:100, R&D Systems, Abingdon, UK), integrin α5 (1:100, CD49e, BD Pharmingen, NJ, USA), integrin β1 (1:100, CD29, BD Pharmingen, NJ, USA), fibronectin (1:100, Chemicon Millipore, Watford, UK), collagen IV (1:100, AbD SeroTec, Oxford, UK) and phage display anti-heparan sulfate antibody HS4C3V (kindly provided by T. H. van Kuppevelt, Nijmegen, The Netherlands) (Thompson et al., 2009) detected by rabbit anti-VSV-G tag IgG (Abcam, Cambridge, UK).

Detection of *lacZ*

P5 eyes were fixed in 1% PFA in PBS for 24 hours at 4°C. Retinas were dissected and incubated in detergent (2 mM $MgCl_2$, 0.01% sodium deoxycholate, 0.02% Nonidet P-40 in PBS) twice for 20 minutes at room temperature followed by overnight incubation at 37°C in staining solution (2 mM $MgCl_2$, 0.01% sodium deoxycholate, 0.02% Nonidet P-40, 5 mM potassium ferricyanide, 5 mM potassium ferrocyanide in PBS) containing 1 mg/ml X-gal (Sigma-Aldrich, Dorset, UK). After colour development, retinas were rinsed in detergent and PBS before counterstaining with fibronectin.

Intraocular injection of peptides in C57BL/6 pups

Two peptides were generated by the Peptide Synthesis Laboratory (Cancer Research UK). Peptide $FNIII_{13-14}$ is derived from the vitronectin heparin-binding sequence that inhibits VEGFA binding to the Hep-II domain of FN. A comparable heparin-binding peptide derived from the A domain of von Willebrand factor that does not inhibit binding of VEGFA to the Hep-II domain of FN was used as controls (Wijelath et al., 2006). The sequences and IC_{50} values for peptide inhibition of FN-VEGF binding are as follows: $FnIII_{13-14}$, AKKQRFRHRNRKGYR, IC_{50} 0.08 μM; Fn control, KDRKRSELRRIASQVK, IC_{50} 250 μM.

Peptides were dissolved in distilled H_2O and prepared freshly for each experiment. Inhibitory concentration was calculated according IC_{50} and a total volume of maximal 0.5 μl of $FnIII_{13-14}$ and control peptides were injected once intraocularly under isoflurane anaesthesia in C57BL/6 pups at P4. Eyes were collected 15-24 hours later. Injections were performed using 10 μl gas-tight Hamilton syringes equipped with 34 gauge needles attached to a micromanipulator. Eyes were fixed in 4% PFA for immunofluorescent staining or snap frozen on dry ice for protein analysis.

PI3 kinase activity assay

Assays on PI3K isolated from retinas were performed as previously described (Graupera et al., 2008). Briefly, total protein lysate of P5 retinas was immunoprecipitated using phosphotyrosine peptide (p-peptide) matrix YPVPMLG (where YP is phosphotyrosine – the YPVPMLG peptide contains the consensus binding sequence for the SH2 domain of the class IA PI3K regulatory subunits). Kinase assays were performed using phosphatidylinositol-4,5-bisphosphate [PtdIns(4,5)P_2; Lipid Products, Redhill, Surrey, UK] as a substrate. Radioactivity in the phosphatidylinositol-3,4,5-trisphosphate [PtdIns(3,4,5)P_3] spot was measured by a Molecular PhosphorImager FX (Bio-Rad, Hercules, CA) and expressed as arbitrary units. The activity present in the control IgG immunoprecipitates was subtracted from that found in IRS immunoprecipitates.

SDS gel electrophoresis and western blotting

Eyes were harvested from pups and immediately dissected in PBS. Any excessive liquid was removed, retinas snap-frozen on dry ice and stored at –80°C.

Whole-retina protein lysates were obtained in radioimmunoprecipitation assay (RIPA) buffer [50 mM Tris-HCl (pH 7.5), 150 mM NaCl, 1 mM EDTA, 1% Nonidet P-40, 0.25% Na-deoxycholate] containing Complete protease inhibitor cocktail (1 tablet/10 ml RIPA, Roche, Welwyn Garden City, Hertfordshire UK) and phosphatase inhibitor cocktail (1:100, Sigma-

Aldrich, Dorset, UK). Equal amounts of protein containing 4× loading buffer (NuPAGE LDS, Invitrogen, Renfrew, UK) and reducing agent β-mercaptoethanol (final concentration 2.5%) were heated at 70°C for 10 minutes and separated on 4-12% NuPAGE Novex Bis-Tris gel according to the manufacturer's instructions.

Primary antibodies were incubated in 2% BSA/ TBS-T containing 0.02% sodium azide at 4°C overnight. After washing the membrane, HRP-conjugated secondary antibodies were incubated in 2% milk powder/TBS-T for 2 hours at room temperature and detected using chemoluminescence ECL reagents (Amersham, GE-Healthcare, Buckinghamshire, UK). Antibodies used were: pVEGFR2 (1:1000, Cell Signaling Technology, Danvers, MA), VEGFR2 (1:1000, Cell Signaling Technology, Danvers, MA), β-tubulin (1:3000, Covance distributed by Cambridge Bioscience, Cambridge, UK), p-Ser478 AKT (1:1000, Cell Signaling Technology, Danvers, MA) and AKT (1:1000, Cell Signaling Technology, Danvers, MA).

Densitometric quantification

Developed films were scanned, images were then analysed using ImageJ and applying uncalibrated optical density (grey value). Band sizes were measured and normalized to the appropriate control gene.

Confocal microscopy

Confocal laser scanning microscopy was performed using a Zeiss LSM 510 Meta microscope. Objectives used were: 63× water immersion NA1.2 C-APOCHROMAT, 40× water immersion NA1.2, C-APOCHROMAT, 25× water immersion NA0.8 Plan-NEOFLUAR and 2.5× NA0.075 Plan-NEOFLUAR. Images were processed using Volocity (Improvision, Coventry, UK) and Adobe Photoshop.

Quantification of retinal parameters

For vessel density measurement, branch points per visual field (200×200 μm) were counted using ImageJ. Migration of vessels was analysed by measuring the radial distance from the optic nerve head to the vascular front at the retinal periphery.

The relative migratory distance of vessels per 24 hours upon treatment with blocking peptides was estimated by setting the day 4 average distance of control eyes as the baseline, which was subtracted from the actual measurement of treated and control eyes obtained at day 5.

The number of filopodia per 100 μm leading endothelial vessel membrane was assessed on 40× confocal micrographs (at least four randomly selected front areas per retina and at least four mice/genotype).

Statistical analysis

Statistical analysis was performed with Prism 5.0a software (GraphPad Software, San Diego, CA) using a two-tailed, unpaired *t*-test. $P \leq 0.05$ was considered to be statistically significant.

ERK and VEGFR2 analyses

Human umbilical vein endothelial cells (HUVECS) were obtained from Cascades Biologics and were maintained in MCDB-131 medium containing low serum growth supplement (Invitrogen). VEGFA was obtained from R&D Systems.

^{125}I-VEGF solid-phase binding assay

A peptide competition assay with ^{125}I-VEGF was performed with recombinant FN $(III)_{9\text{-}10/12\text{-}14}$ immobilized on the plate as previously described (Wijelath et al., 2002). HUVECS were cultured in 60 mm culture dishes in MCDB-131 growth medium until 80% confluent. Cells were then washed and incubated for 4 hours in serum-free MCDB-131 medium, before stimulation with VEGF (5 ng/ml). $FNIII_{13\text{-}14}$ peptides were incubated with VEGF for 5 minutes at 37°C before adding to cultures. For ERK phosphorylation, cultures were stimulated for 5 minutes. For VEGFR2 phosphorylation studies, cultures were stimulated for 3 minutes. Detection and analysis of ERK and VEGFR2 phosphorylation were performed as described previously (Wijelath et al., 2006).

Migration assay was performed as described previously (Ishida et al., 2001). HUVECs were treated with inhibitory peptides (increasing concentration: 5, 25, 50 and 100 μM) and incubated for 4 hours before counting the number of cells migrated in response to VEGF (20 ng/ml). Data are representative of two separate experiments, each carried out in triplicate.

Quantification of immunofluorescence intensity

Quantification was performed using the 'surface' function of Imaris software to determine total pixel intensity of FN immunofluorescent staining associated with blood vessels or ACs. Vessels volume was measured using 'surface' function of isolectin-B4 staining. Area of ACs was ascertained by subtraction of vessel volume from the total image area (1024×1024, 16 bit). Images were taken with 40× objective lens using a Laser Scanning Microscope 510 (Zeiss). Statistical analysis was performed using GraphPad Prism 5.0c.

RESULTS

Fibronectin localization in the retinal vasculature

Visualization of FN by immunofluorescence staining revealed FN localization on ACs ahead of the growing vessels at postnatal day 5 (P5) in the mouse retina (Fig. 1A-C). Co-labelling with PDGFRα, a cell-surface receptor specifically expressed on ACs (blue, Fig. 1D), and staining with isolectin B4 (green) to visualize endothelial cells (EC) confirmed the specificity of astrocytic FN expression ahead of the vessels and in ACs closely associated with the vasculature (Fig. 1C,D).

Uemura et al. reported FN expression by in situ hybridization on ACs ahead of the growing vasculature (Uemura et al., 2006). In addition, RT-PCR of FACS-sorted retinal endothelial and astrocytic cell fractions revealed FN expression in both cell types (Uemura et al., 2006). We observed fibrillar FN assembly over the entire astrocytic network ahead of the vessels (arrows in Fig. 1A-C). Interestingly, FN expression was significantly reduced on ACs when vascular sprouts have grown over the astrocytic network (Fig. 1A). Thus, astrocytic FN could provide a transient matrix for endothelial tip-cell guidance.

Higher magnification imaging revealed that extended filopodial protrusions closely align to the FN-rich astrocytic network (arrows, Fig. 1B). In marked contrast to the FN distribution, we find collagen IV (red, Fig. 1E,F), a major BM component localized along retinal vessels forming a continuous layer surrounding ECs of established vessels (Fig. 1E). Tip cells and their filopodia lack a continuous collagen IV BM (Fig. 1F).

Astrocytic FN provides a guidance matrix for growing vessels

To study the function of astrocytic FN, we specifically deleted FN from ACs by Cre-lox-mediated recombination of the floxed FN allele (Sakai et al., 2001). For this purpose, we used mice expressing Cre recombinase under the control of the glial fibrillary acidic protein (GFAP) promoter (Bajenaru et al., 2002). The bicistronic GFAP::Cre-IRES-LacZ-NLS transgene allows monitoring the promoter activity by nuclear Xgal staining (Fig. 2A-C). Counterstaining of FN (red, Fig. 2B,C) in the absence of the floxed FN allele revealed GFAP promoter activity in FN-expressing ACs ahead of the growing vascular plexus (arrowheads, Fig. 2C) and in ACs closely associated with the vasculature (arrows, Fig. 2C), indicating that the GFAP transgene driving Cre is efficiently and specifically expressed by retinal ACs.

GFAP Cre+ $FN^{flox/flox}$ mice, referred to as FN^{ACko}, revealed a strong reduction of FN expression in ACs (judged by immunofluorescence staining, Fig. 2E,H). Immunofluorescence staining with FN (red) illustrated astrocytic FN deposition ahead of the growing vasculature in control retinas (Fig. 2D,G). whereas astrocytic FN is markedly (Fig. 2E,H) or significantly (Fig. 2F,I) reduced in FN^{ACko} retinas. Retinas in which GFAP Cre-mediated recombination has effectively deleted FN from most ACs display absent/reduced FN ahead of the vessels (Fig. 2K,H) and also show

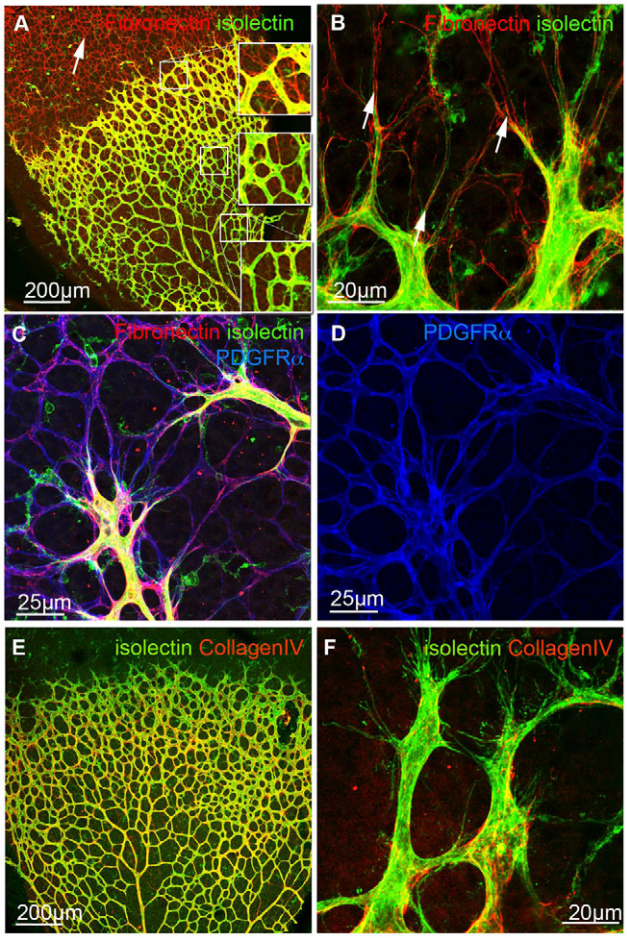

Fig. 1. Localization of extracellular matrix component FN and collagen IV in the retinal vasculature. (**A-D**) Immunofluorescence staining for fibronectin (FN, red A-C) revealed strong deposition ahead of the growing vasculature (white arrow, A), whereas astrocytic FN expression is reduced in the mature vascular plexus. Boxed areas in A are shown at higher magnification, demonstrating the lack of astrocytic FN deposition (red) in the mature retinal vascular plexus. Blood vessels were visualized with isolectin-B4 (green, A-C) and co-labelling with PDGFRα (blue, C,D) confirmed astrocytic deposition of FN. Note that the apparent vascular staining with PDGFRα reflects astrocytic endfeet in close association with the blood vessels. High magnification imaging showed alignment of filopodia to astrocytic matrix (arrows, B). (**E**,**F**) In contrast to FN, collagen IV (red) is distributed in the abluminal BM of retinal vessels (green, E) and absent from endothelial tip cells and filopodia (F). High magnification images are projections of confocal *z*-stacks encompassing the depth of the vasculature.

prominent reduction of FN localization around blood vessels (Fig. 2E,H), suggesting that ACs are a significant source of perivascular FN in the retina. Given that ECs, pericytes (PC) and AC endfeet are closely juxtaposed, and that ECs and PCs share a BM, we decided to investigate directly the relative FN contribution by conditional deletion in the three compartments. Tamoxifen-inducible EC and constitutive PC specific deletion was achieved using the PdgfbiCre (Claxton et al., 2008) and PdgfrbCre (Foo et al., 2006) lines, respectively. We analysed FN expression in P5 retinas in EC (FN^{ECko}), PC (FN^{PCko}), AC (FN^{ACko}) and compound EC/PC ($FN^{EC/PCko}$), as well as in AC/EC ($FN^{AC/ECko}$)-specific deletion (see Fig. S1A-F in the supplementary material). Recombination in EC was achieved by tamoxifen injection at P2 and P3. The results confirmed prominent loss of AC FN and perivascular FN labelling in FN^{ACko}, with no further reduction in $FN^{AC/ECko}$ (see Fig. S1A-C,G in the supplementary material). By contrast, FN^{ECko}, FN^{PCko} and $FN^{EC/PCko}$ showed no significant loss of perivascular FN (see Fig. S1D-F,H in the supplementary material), together indicating that AC FN can fully compensate for EC and PC deletion, and that, in the retina, AC provide a major source of FN.

Heterozygous $FN^{flox/+}$ GFAP Cre+ ($FN^{ACko/+}$) mice showed intermediate reduction of astrocytic FN staining, illustrating a quantitative correlation between allelic contribution and FN protein deposition (data not shown). Counterstaining for astrocytic PDGFRα (blue, Fig. 2J-L) illustrated that network formation and morphology of ACs was not affected by loss of FN (red, Fig. 2J-L).

High-magnification images revealed robust fibrillar FN assembly on ACs and in the endothelial BM of control mice (Fig. 2M). In FN^{ACko} mice, astrocytic FN protein staining was reduced to small traces, leaving large parts of the astrocytic cell surface free of FN fibrils (arrowheads, Fig. 2N). Mosaic recombination produced regional residues of astrocytic FN (arrows, Fig. 2L,N,O). Endothelial filopodia elongated along ACs in regions of high fibrillary FN (Fig. 2O). In the absence of astrocytic FN, however, endothelial filopodia appeared conspicuously short and bundled in broad bursts of excessively numerous extensions (Fig. 2N, asterisks), suggesting that astrocytic FN may play a role in filopodial adhesion and possibly tip-cell migration.

In support of this hypothesis, we consistently observed a small but significant reduction in the radial expansion of the vascular plexus in FN^{ACko} in comparison with littermate controls (Fig. 3A,B). Radial expansion is mainly driven by endothelial tip-cell migration, indicating that astrocytic FN promotes tip-cell migration. The radial distance of vessel migration (Fig. 3C) in retinas of FN^{ACko} and $FN^{ACko/+}$ when compared with control (ctrl) littermates was delayed by 9% in FN^{ACko} and by 5.5% in $FN^{ACko/+}$. Regions of complete FN deletion generally showed stronger reduction (see Fig. S2 in the supplementary material), suggesting that the mean reduction measured across the retinal samples underestimates the full magnitude of the migratory defects caused by FN deficiency. Quantification of morphological parameters of the growing vascular plexus confirmed the impression of increased numbers of filopodia (Fig. 3D) extending at the vascular front. In addition, branch points were increased by 35.5% in the plexus of FN^{ACko} compared with control littermates (Fig. 3E). In addition, the diameter of vessels appeared slightly increased (Fig. 2N), together suggesting that endothelial cell proliferation as well as sprouting and branching activity is not reduced in parallel to the reduced radial expansion of the vascular plexus.

Although we observed considerable GFAP promoter activity and Cre-mediated recombination of the floxed FN allele in ACs ahead of the vascular plexus (Fig. 2A), GFAP promoter activity was sharply increased in ACs in contact with the developing vascular plexus (Fig. 2A-C). Earlier studies also showed by in situ hybridization that GFAP expression is weak in ACs that invade the retina at P0 (in the absence of retinal blood vessels) and becomes strongest in mature ACs associated with the vasculature in the centre of postnatal (P5) retinas (Chu et al., 2001; Fruttiger, 2002). This late onset of the GFAP promoter combined with FN protein stability could be the cause of the observed residual astrocytic FN, potentially masking a more fundamental role of astrocytic FN in vascular patterning. To address whether the delay of vessel

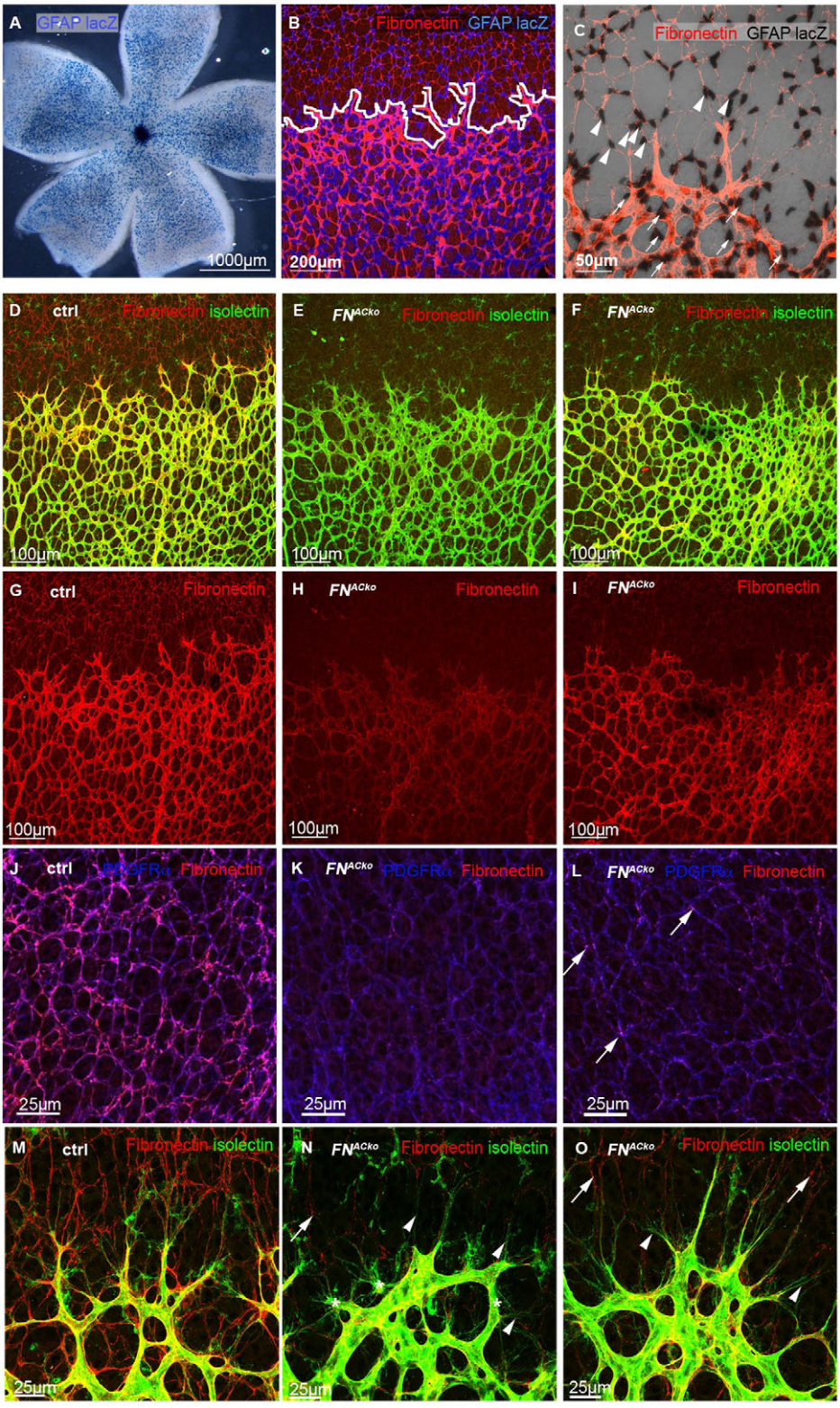

Fig. 2. GFAP Cre specifically and efficiently ablates FN expression in ACs ahead of the sprouting vascular front. (**A-C**) Visualization of nuclear GFAP *lacZ* (blue, A,B; black, C) revealed GFAP promoter activity in P5 retina (A). Border between ACs and vasculature is indicated by white line (B), as illustrated by co-labelling with fibronectin (red, B). High magnification imaging of the sprouting vascular front revealed GFAP *lacZ* expression in ACs ahead of vessels (arrowheads, C) and in ACs surrounding the vascular plexus (arrows, C) visualized by FN staining (red). High magnification images are projections of confocal *z*-stacks encompassing the depth of the vasculature. (**D-I**) GFAP Cre-mediated deletion of AC-derived fibronectin (FN^{ACko}) leads to reduced FN expression in mutant retinas (E,F) compared with control retinas (ctrl, D), as shown by FN immunofluorescence staining (red, D-I). (**J-L**) Counterstaining of ACs with PDGFRα (blue) and FN (red) reveals normal network development but reduced FN deposition in FN^{ACko} (K,L) compared with control littermates (J). White arrows indicate residual FN expression in FN^{ACko} retinas in the astrocytic network ahead of the vasculature (red, L) and sprouting vascular front (red) resulting in mosaicism. (**M-O**) High-magnification images showing the absence of astrocytic FN ahead of the sprouting vascular front in FN^{ACko}. Arrowheads indicate regions with complete loss of FN (N,O). Deficiency of astrocytic FN matrix leads to aberrant filopodia extension (asterisk, N). Arrows in N and O indicate regional residues of astrocytic FN.

migration is enhanced when FN is deleted in AC progenitors before retinal vascularization, we crossed FN floxed mice to the NesCre8 line, expressing Cre recombinase under the Nestin promoter (Petersen et al., 2002). Nestin is an intermediate filament transiently expressed by dividing and migrating cells of the developing CNS and is later replaced by cell-type-specific intermediate filaments such as GFAP (Beech et al., 2004). At P5, vessel migration in $NesCre^{+}$ $FN^{flox/flox}$ mice was reduced by 12% (see Fig. S3A-C in the supplementary material). Immunostaining of FN (green, see Fig. S3D-G in the supplementary material) revealed a substantial loss of FN in the astrocytic network and in the vascular compartment. However, residual FN on ACs prevailed, suggesting that plasma FN might assemble on ACs and contribute to a minor extent to the astrocytic FN matrix. The

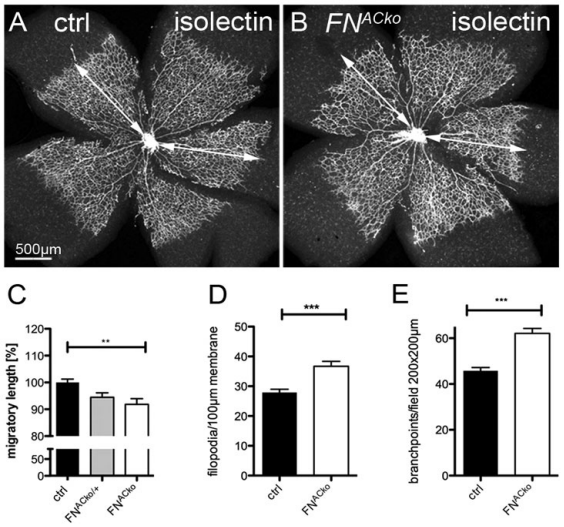

Fig. 3. Loss of astrocytic FN results in reduced migration of vessels. (**A**,**B**) Visualization of the retinal vasculature (P5) by isolectin-B4 immunofluorescence staining revealed reduced migration towards the retinal periphery in mice deficient of astrocytic FN. Vessel migration was quantified by measuring total length as illustrated by the white arrow (A,B). (**C**) Radial expansion of superficial vessels at P5 in control (n>5), heterozygous ($FN^{ACko/+}$, n>3) and FN^{ACko} mice (n>5). $^{**}P$<0.01 one-way ANOVA. Values represent mean+s.e.m. (**D**) The number of filopodial protrusions per vessel length at the migrating vascular front of P5 mice (n≥20). $^{***}P$<0.0001. Values represent mean+s.e.m. (**E**) The number of branch points per image field of P5 FN^{ACko} and control mice, n≥10. $^{***}P$<0.0001. Values represent mean+s.e.m.

greater migration defect in Nestin Cre-positive mice compared with the FN^{ACko} is therefore likely to be a consequence of an earlier reduction of astrocytic FN from the very beginning of retinal vascular development, rather than a more complete recombination in all ACs.

In addition to reduced vessel migration, and similar to FN^{ACko} retinas, $NesCre^{+}$ $FN^{flox/flox}$ retinas displayed increased filopodia formation, branching and vessel density, as well as increased vessel diameter (see Fig. S3H,I in the supplementary material). These results suggest that astrocytic FN promotes tip-cell migration and filopodial elongation.

The FN-binding domain RGD is not required for vessel migration

Fibronectin binds to integrin α5β1 via the RGD (Arg-Gly-Asp)-binding domain and thereby mediates cell attachment. Using antibodies directed against integrin α5 or integrin β1, we confirmed that both integrins are expressed by ECs and predominantly localized at the abluminal endothelial cell surface facing the BM of retinal vessels (see Fig. S4A-F in the supplementary material). High magnification revealed a spotty localization of integrin β1 (see Fig. S4A-C in the supplementary material) and integrin α5 (see Fig. S4D-F in the supplementary material) on filopodia of leading tip cells (arrows). In addition, integrin β1 is expressed by pericytes and in vascular smooth muscle cells (Abraham et al., 2008).

To investigate whether the regulation of endothelial tip-cell morphology and migration by astrocytic FN requires fibronectin ligation of integrins, we took advantage of a mouse line, in which the RGD-motif of FN was replaced by an inactive RGE motif, thus inhibiting the binding of FN to integrin α5β1 and αvβ3. $FN^{RGE/RGE}$ homozygous mice are embryonic lethal and embryos display severe vascular defects (Takahashi et al., 2007), resembling the phenotype of α5 integrin (*Itga5*)-deficient mice (Yang et al., 1993). We crossed FN^{ACko} mice with heterozygous $FN^{RGE/wt}$ mice to obtain FN^{ACko}/RGE mice. These mice are viable as they produce wild-type FN from one floxed allele in all GFAP-Cre negative cells, in addition to FN RGE from the second allele. GFAP-expressing retinal ACs, however, recombine the floxed FN allele, thus producing only FN RGE lacking the integrin-binding site.

We then analysed the retinal vasculature and the migratory length of vessels, as well as FN assembly. Radial expansion of retinal vessels was not affected in $FN^{RGE/wt}$ mice compared with control littermates (Fig. 4A-C). FN^{ACko}/RGE mice showed a small but significant 5% reduction in radial expansion, which is identical to that observed in the astrocyte-specific heterozygous $FN^{ACko/+}$ mice (Fig. 3C). Together, these observations suggest that astrocytic FN promotes endothelial migration in a gene dose-dependent manner, independent of RGD-mediated integrin binding.

However, close examination of endothelial tip cells and alignment of filopodia along the FN-rich astrocytic network revealed an increased number of mis-aligned filopodia in FN^{ACko}/RGE (arrowheads, Fig. 4I) compared with control littermates (Fig. 4G), suggesting a role of integrin-FN interaction in filopodial alignment or stabilization. Analysis of confocal *z*-stacks revealed aberrant endothelial filopodial protrusions in FN^{ACko}/RGE retinas below the astrocytic FN-matrix level (see Fig. S5C-C″″ in the supplementary material), possibly as a consequence of reduced interaction of filopodia with the mutant FN protein.

Immunofluorescence staining (green, Fig. 4I) revealed astrocytic FN in FN^{ACko}/RGE retinas, confirming previous reports that the absence of a functional RGD motif in FN still permits assembly of a FN matrix in mutant embryos or on mutant cells (Takahashi et al., 2007). However, we observed a patchy and less fibrillar deposition of astrocytic FN ahead of the vasculature in FN^{ACko}/RGE retinas (Fig. 4I; see Fig. S5C-C‴ in the supplementary material), whereas FN on blood vessels appeared equally fibrillar as in control retinas (arrows, Fig. 4I). It is possible that a distinctive assembly of the mutant FN via alternative integrin-binding domains may compromise filopodia interactions with the astrocytic FN matrix.

In order to investigate further the role of FN-integrin interaction in tip-cell migration, we studied retinas from mice lacking endothelial integrin α5 expression. Unlike germline deletion of *Itga5*, endothelial-specific deletion of *Itga5* using Tie2-Cre (van der Flier et al., 2010) leads to surprisingly normal vascular development in the postnatal mouse retina (Fig. 4D,E). However, high magnification analyses of leading endothelial tip cells also displayed filopodial misalignment (arrows, Fig. 4H; Fig. S5B-B″″ in the supplementary material) similar to the alignment defects observed in FN^{ACko}/RGE (Fig. 4I), together indicating poor adhesion of endothelial cells to the astrocytic scaffold. Radial migration (summarized in Fig. 4F) was marginally reduced by 3-6%, confirming that endothelial tip-cell migration is surprisingly independent of endothelial integrin α5β1 interaction with astrocytic FN.

Decreased VEGFR2 signalling and PI3 kinase/AKT activity in the absence of astrocytic FN

A recent study reported that binding of VEGF to the heparin II domain of FN is necessary for optimal VEGF-induced endothelial cell proliferation, migration and ERK activation in vitro (Wijelath et al., 2006). To address whether the reduced migration in FN^{ACko} is a consequence of decreased VEGF signalling, we analysed

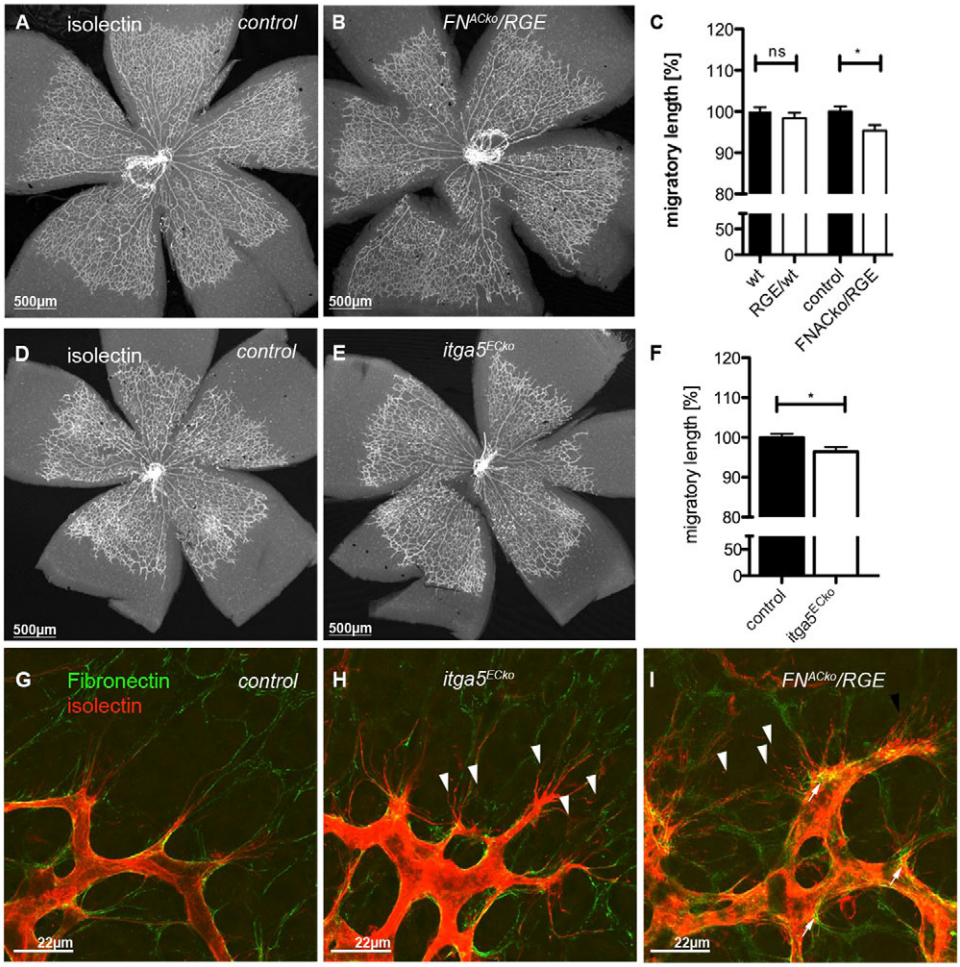

Fig. 4. RGD integrin binding in FN is dispensable for retinal migration but promotes filopodial alignment. (**A**,**B**) Mutation of integrin-binding RGD to an inactive RGE motif in astrocytic FN (*FN^{ACko}/RGE*) does not affect radial expansion of vessels towards the periphery and overall vascular patterning. (**C**) Vessel migration in RGE/wild-type mice and mice inheriting inactive RGE motif in astrocytic FN: wild type and RGE/wild type (n>8); control and *FN^{ACko}/RGE* (n=5). *P<0.05. Values represent mean+s.e.m. (**D**,**E**) Overview images of the retinal vasculature of mice deficient in endothelial integrin α5 (*Itga5^{ECko}*, E) illustrates no significant defects in vessel morphology compared with control littermates (D). (**F**) Retinal vessel migration of control and *Itga5^{ECko}* mice at P5. Number of mice: control, n=9; *Itga5^{ECko}*, n=6. *P<0.05. Values represent mean+s.e.m. (**G-I**) High-magnification imaging of filopodia (red, G-I) at leading tip cells displayed mis-alignment of filopodia to the astrocytic FN matrix (green) in mice deficient for endothelial Itga5 (H) and mice lacking astrocytic FN RGD (I) when compared with control mice (G). Arrowheads indicate misaligned filopodia.

VEGF receptor 2 (VEGFR2) activation by western blot. Total protein extracts of P5 retinas were analysed for VEGFR2 phosphorylation. Despite similar levels of VEGFR2 protein expression, VEGFR2 phosphorylation was strongly reduced in *FN^{ACko}* compared with control retinas (Fig. 5A), suggesting that FN is also essential for VEGF signalling in vivo.

Downstream of VEGF-VEGFR2 activation, the class IA phosphoinositide 3-kinases (PI3K) signal via AKT and downstream effectors to regulate endothelial cell migration (Graupera et al., 2008). PI3K activity was significantly reduced by ~25% in *FN^{ACko}* retinas (Fig. 5B). Western blot analysis demonstrated a marked reduction in AKT phosphorylation at Ser473 (Fig. 5C), suggesting that FN promotes tip cell migration by stimulating VEGFR2 signalling and downstream PI3K/AKT activation.

Interestingly, mice lacking endothelial integrin α5 (*Itga5*) express comparable levels of activated AKT to their control littermates (Fig. 5C,D), indicating that VEGFR2 signalling is unaffected in *Itga5^{ECko}* mice. These results suggest that the reduced radial expansion in *FN^{ACko}* retina is a consequence of diminished VEGFR2 signalling and occurs independently of α5β1-integrin-mediated interaction.

Inhibition of VEGF binding to FN impairs retinal vascularization

How astrocytic FN promotes VEGF and downstream signalling remains unclear. To examine directly whether FN-VEGF binding is required for retinal vessel expansion, we took advantage of peptides that inhibit the binding of VEGF to fibronectin (Wijelath et al., 2002) (Fig. 6A). In cell culture experiments using human umbilical vein endothelial cells (HUVECs) plated on FN, the addition of peptide FnIII$_{13-14}$ significantly inhibited VEGFA-induced VEGFR2 phosphorylation (Fig. 6B) and downstream extracellular-signal regulated kinase (ERK) signalling (Fig. 6C), as well as endothelial cell migration, in a dose-dependent manner (Fig. 6D), These results suggested that the inhibition of VEGF binding to FN can directly translate into reduced migration. To address whether this finding holds true in vivo, we administered FnIII$_{13-14}$ (Wijelath et al., 2006) peptides by intraocular injection (Gerhardt et al., 2003) in postnatal C57BL/6 pups. Twenty-four hours post-injection, we harvested eyes to analyze retinal vessel development. Measuring the radial expansion of vessels, we observed a 10% reduction in eyes injected with FnIII$_{13-14}$ peptides compared with control injected eyes (Fig. 6E). Control peptides did not affect radial expansion when compared with non-injected contralateral eyes. The 10% overall reduction in radial expansion signifies a substantial inhibition of vessel migration given that the peptides were present for only 24 hours, i.e. the fifth day of 5 days of retinal development. On average, vessels migrate 200-250 μm per day towards the retinal periphery. To estimate the acute effect of 24 hours peptide treatment, we reasoned that retinal vessels will have migrated normally before treatment on day 4 and therefore used the average day 4 radius as the baseline to calculate the distance vessels have migrated after injection (Fig. 6F). This representation illustrates that inhibition of FN-VEGF binding by injection of peptide FnIII$_{13-14}$ for 24 hours

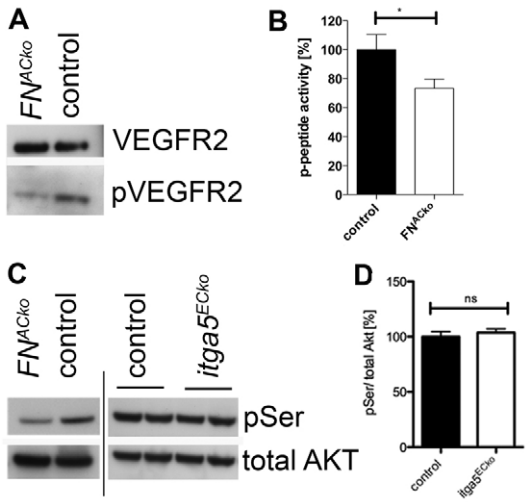

Fig. 5. Loss of astrocytic FN impairs VEGFR2-mediated stimulation of migration via the PI3K pathway. (**A**) Western blot analysis showed reduced phosphorylation of VEGFR2 but not of total VEGFR2 protein levels in retinas of P5 FN^{ACko} compared with control mice. (**B**) PI3K activity determined by pull-down assays with pY-peptides was markedly reduced in FN^{ACko} retinas. Control and FN^{ACko} retinas for p-peptide, n=7. *P<0.05. Values represent mean+s.e.m. (**C**) Phosphorylation of serine residue 473 (pSer) of AKT relative to total levels of AKT was significantly reduced in FN^{ACko} retinas (C) but not in $Itga5^{ECko}$ retinas (C). (**D**) Densitometric analyses of P5 control (n=4) and Itga5 retinas (n=5). Values represent mean+s.e.m.

reduced vessel migration by almost 40%, whereas control peptides had no effect. $FnIII_{13-14}$ peptide injection also led to reduced pVEGFR2 and pSer-AKT levels (Fig. 6G,H), suggesting that the inhibition of VEGF-binding impairs vessel migration by limiting VEGFR2 and PI3K/AKT signalling.

Heparan sulfate synergizes with FN in VEGF binding

As FN is not the only matrix component with known VEGF-binding ability, we investigated AC expression of heparan-sulphate (HS) proteoglycans. Using epitope selective phage-display antibodies (Thompson et al., 2009), we observed abundant labelling of ACs ahead of, and around, forming vessels in the retina (Fig. 7A-C). Higher magnification revealed distinct fibrillary staining on AC, highly reminiscent of the FN pattern (Fig. 7B). Thus, it is possible that AC deficient in FN are still able to retain some of their cell-surface VEGF-binding capacity mediated by HS interactions (Joyce et al., 2005; Jakobsson et al., 2006; Hawinkels et al., 2008). In order to understand the functional importance of AC HS, we deleted the key glycosyltransferase Ext1, which is required for elongation of the disaccharide side-chains of HS proteoglycans, selectively in ACs. Using the GFAP Cre mice and the floxed alleles of the Ext1 and the FN gene, we generated mice deficient in AC Ext1 ($Ext1^{ACko}$), and deficient in both AC FN and Ext1 ($FN/Ext1^{ACko}$). Deletion of AC Ext1 led to a 15% reduction, whereas deletion of AC Ext1 and FN caused a reduction of 32%, in radial expansion compared with littermate controls (Fig. 7D-H). Together, the similarity in expression patterns of AC FN and HS, and the additive effect of compound deletion, suggest that both components synergize in VEGF-binding to support directed migration of endothelial tip cells.

DISCUSSION

The present study provides insights into the function of extravascular scaffolds of FN during angiogenesis. Unlike the global deletion of FN or one of its major integrin receptors, α5β1, which leads to early embryonic cardio-vascular failures, the selective deletion of FN from cells that provide a migratory scaffold for endothelial cells reveals a role of FN in quantitatively modulating endothelial VEGFR signalling and downstream PI3K activity to enhance endothelial tip-cell migration. Endothelial-specific deletion of the major FN receptor, integrin α5, or selective replacement of wild-type FN containing the integrin-binding RGD sequence with an inactive RGE mutant in ACs, illustrate that FN scaffolds perform two distinct functions on endothelial sprouts (summarized in Fig. 7H); integrin-mediated filopodial alignment and VEGF binding promoting VEGFR/PI3K signalling in tip-cell migration.

FN is an excellent migration substratum for endothelial cells and is abundantly present in the early embryo during vascular development (Risau and Lemmon, 1988). FN is present as soluble protein in plasma (Sakai et al., 2001) and is produced by epithelial, endothelial and many mesenchymal cells, underlining its important function in embryogenesis and organogenesis. This wide distribution also makes it difficult to isolate specific functions of locally produced FN. Early studies reported FN expression in cultured brain astroglia and astroglioma, but not in healthy adult or developing brain astroglia (Liesi et al., 1986; Halfter et al., 1989). FN expression by ACs has been implicated in retinal angiogenesis (Jiang et al., 1994; Uemura et al., 2006), but the functional relevance remained unclear. Mice deficient in the orphan nuclear receptor tailless (Tlx) display severe delays and patterning defects in retinal vascularization (Uemura et al., 2006). Astrocytes lacking Tlx show poor FN assembly, indicating that lack of astrocytic FN abrogates retinal vascular development. Our current data represent the first functional analysis into the role of astrocytic FN in this process. The significant, but relatively small delay in radial expansion, with largely intact overall pattern formation, suggests that the severe defects observed in *Tlx*-null mice are caused by additional mechanisms that are independent of FN.

High-magnification imaging illustrated that endothelial tip-cell filopodia align with astrocytic FN fibrils. Whereas filopodial formation itself is not stimulated by astrocytic FN, as tip cells in FN^{ACko} produce even more filopodia, their alignment to the astrocytic network and possibly the subsequent adhesion of filopodia and endothelial tip cells to the astrocytic scaffold appear to involve FN-integrin-receptor binding. The major FN receptor, integrin α5β1, is localized at endothelial tip cells and filopodia in the postnatal retina. Surprisingly, selective ablation of *Itga5* in endothelial cells, in marked contrast to global deletion in all cell types, is compatible with embryonic development, functional vascular patterning and vessel morphology (van der Flier et al., 2010). EC loss of *Itga5* caused only marginal delay in retinal vessel migration, suggesting that radial expansion of the retinal plexus is independent of the major FN receptor integrin α5β1. This conclusion is further supported by our analysis of mice bearing an astrocyte-specific replacement of the RGD integrin-binding motif. In FN^{ACko}/RGE retinas, radial migration is indistinguishable from that in $FN^{ACko/+}$ retinas, indicating that the FN RGE protein is equally capable of promoting radial expansion as the wild-type FN protein. Importantly, neither the loss of endothelial integrin α5 nor of the RGD-binding motif substantially compromises FN assembly, probably because alternative binding sites recognized by integrin αv can assemble FN into fibrils (Takahashi et al., 2007; van der Flier et al., 2010). It is therefore interesting to note that despite the

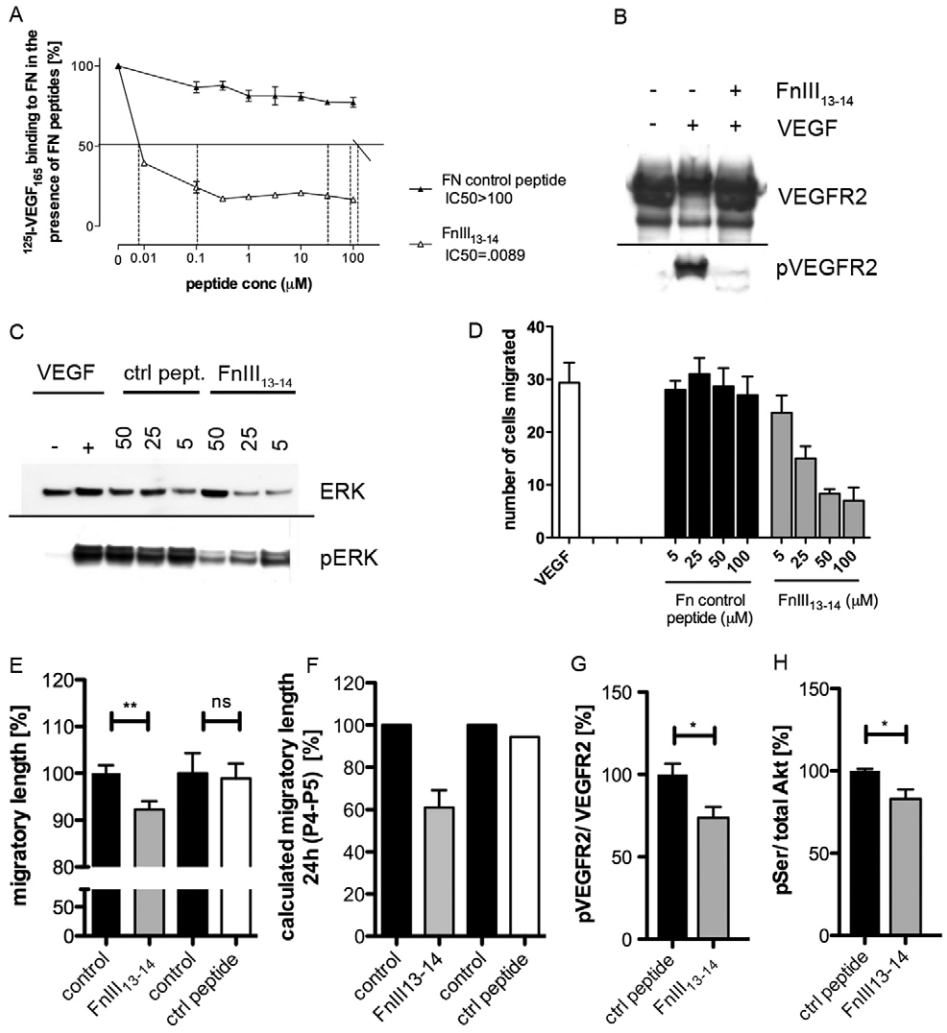

Fig. 6. Inhibition of VEGF binding to FN leads to reduced vessel migration due to decreased VEGFR2 signalling and PI3K activity. (**A**) ^{125}I-VEGF$_{165}$ binding to fibronectin (FN) 9-10/12-14 in the presence of increasing concentrations (μM) of peptides, expressed as a percentage of no-peptide controls (%). The half-maximal inhibitory concentration (IC_{50}) is analyzed to determine the inhibitory function of VEGF binding to fibronectin. (**B**) Control peptides (IC_{50}>100 μM) and FNIII$_{13-14}$ (IC_{50}=0.09 μM) were applied in the following experimental settings. Western blot analyses reveal activation and phosphorylation of VEGFR2 (pVEGFR2) in the presence of VEGF (lane 2). Treatment with inhibitory peptide FNIII$_{13-14}$ abolishes VEGFR2 phosphorylation (lane 3) down to baseline levels obtained in unstimulated conditions (lane 1). VEGFR2 protein levels are comparable in all experimental settings. (**C**) Western blot analyses show that the addition of VEGF results in activation of downstream target pERK whereas ERK protein expression levels are unaffected in the presence of VEGF and varying concentration of FNIII$_{13-14}$ inhibitory peptide. Treatment with increasing concentration of inhibitory peptide FNIII$_{13-14}$ results in concurrent decrease of ERK phosphorylation. (**D**) VEGFA-induced endothelial cell migration was inhibited with increasing concentration of peptide FNIII$_{13-14}$. Control peptide had no effect. Data are mean+s.e.m. (**E**) Distances vessels have migrated towards retinal periphery at P5 when treated with inhibiting peptide FNIII$_{13-14}$ and control peptide for 24 hours compared with uninjected control eyes. By measuring the total length of radial expansion of vessels we determined a significant reduction upon injection of FNIII$_{13-14}$ whereas control peptides have no effects. (**F**) When calculating the distance vessels have migrated during 24 hours of peptide treatment (day P4-P5), we found an almost 40% decrease in vessel migration upon FNIII$_{13-14}$ injection (n>5 injected with FnIII$_{13-14}$; n>5 control peptide injected mice; $^{**}P$<0.01). Values represent mean±s.e.m. (**G**) Phosphorylation of VEGFR2 and AKT were assessed by total protein extraction and western blotting 15 hours after treatment with inhibiting peptides. Densitometric analysis revealed a significant reduction of pVEGFR2 compared with total VEGFR2 expression levels in FnIII$_{13-14}$ injected retinas. (**H**) The percentage of phosphorylated AKT in relation to total amounts of AKT after injection of peptides inhibiting VEGF-FN binding. $^{*}P$<0.05. Values represent mean+s.e.m. (n=7 mice injected with FNIII$_{13-14}$; n=5 control peptide injected mice).

presence of a FN matrix in both the *itga5^{ECko}* and *FN^{ACko}/RGE* retinas, we find abundant filopodial mis-alignment. Thus, any compensatory role of alternative integrin interactions appears not to be able to replace all functions of integrin α5 or of the FN-RGD motif. Nevertheless, this particular phenotype is very subtle and apparently transient, as it does not lead to progressive or persistent vascular defects. The discrete misalignment of filopodia combined with an increased number of filopodia suggests that integrin α5 mediates an adhesive function between tip-cell filopodia and ACs, which might normally promote stabilization of filopodia in contact with the ACs.

Tip-cell migration, in marked contrast to filopodial alignment, is independent of α5β1 integrin, but surprisingly sensitive to the FN abundance. The reduced radial migration in retinas lacking just one

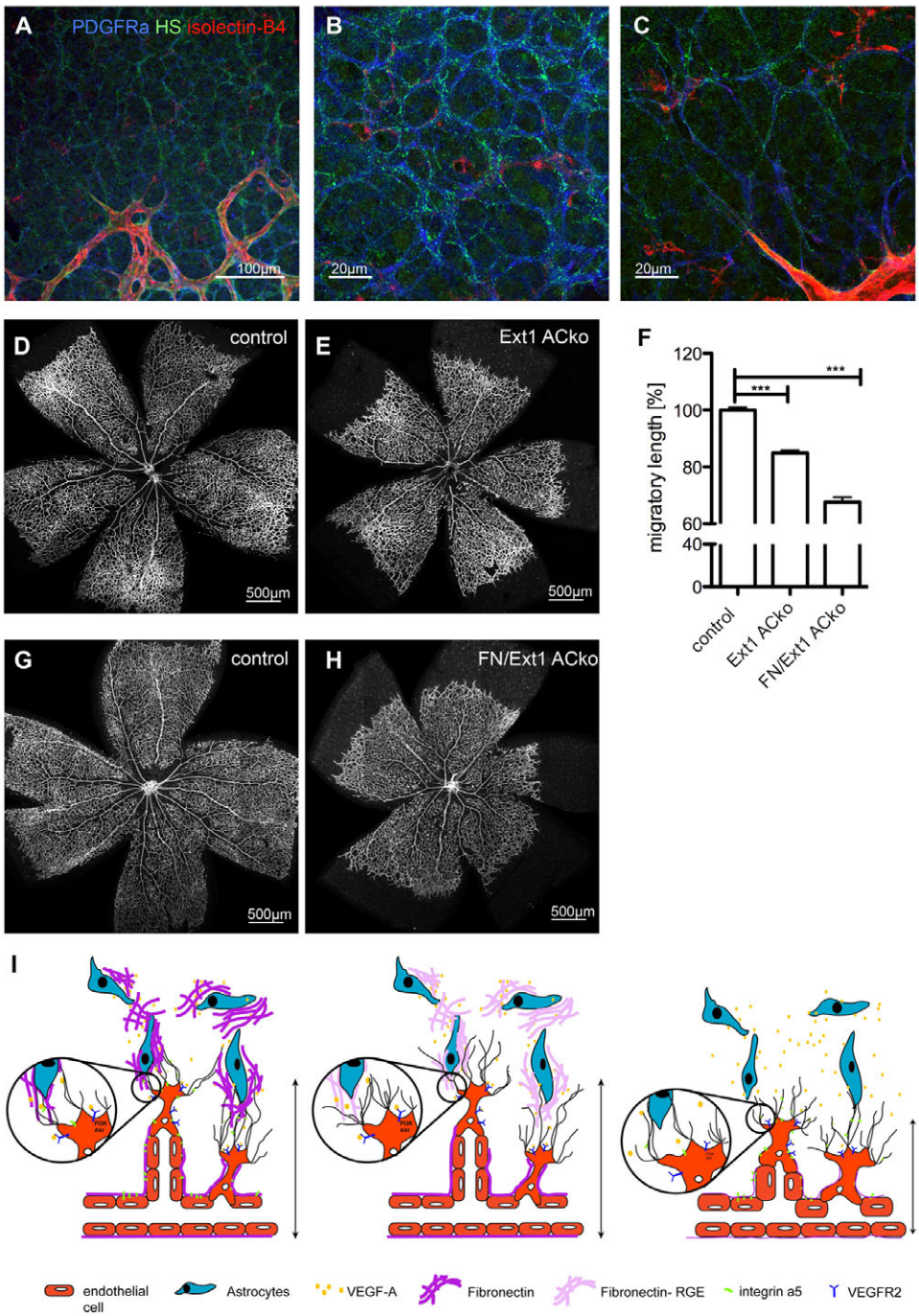

Fig. 7. Compound deletion of astrocytic FN and heparan sulfate (HS) results in an enhanced migratory defect. (**A-C**) Immunofluorescence staining with a phage display antibody (HS4C3V) recognizing sulphated HS chain (green, A-C) revealed a similar expression pattern to that observed for FN (Fig. 1A-C). HS is localized along the astrocytic network ahead of the vasculature (B,C) labelled by the AC marker PDGFRα (blue, A-C). Furthermore, HS is present in the BM surrounding the blood vessels (A,C) visualized by isloectin-B4 (red, A-C). (**D**,**E**,**G**,**H**) Overview images of the retinal vasculature of control mice (D,G), mice deficient in astrocytic HS (Ext1 ACko; E) and mice deficient in both HS and FN (FN/Ext1 ACko; H). (**F**) Percentage of retinal vessel migration at P5 (n>10 control mice; n=6 Ext1 ACko; n=3 FN/Ext1 ACko; ***P<0.0001). Values represent mean+s.e.m. (**I**) Proposed model of astrocytic VEGF-FN interaction regulating vessel migration. Right to left: FN is expressed by ACs ahead of the growing vasculature and assembled in a fibrillar network providing instructive cues for vessel migration. ACs produce and secrete VEGFA in the extracellular milieu and this VEGFA is retained by the FN matrix. Endothelial tip-cell filopodia express integrin receptors that guide filopodial alignment along the ACs and mediate adhesion to the FN matrix. VEGFA binds to VEGFR2 expressed on leading EC, thereby triggering VEGF receptor signalling in tip cells and downstream effectors PI3K. Loss of astrocytic FN results in a diffused VEGFA gradient, reduced VEGF/VEGFR2 signalling and decreased PI3K activity in endothelial tip cells. As a consequence, migration of the vascular plexus is delayed. Selective replacement of integrin RGD-binding motif by an inactive RGE motif in ACs or endothelial-specific deletion of integrin α5 lead to abundant filopodial misalignment and probably to defective tip-cell adhesion. However, in both cases radial vessel migration is not or is only marginal affected. Combined deletion of both matrix components FN and HS from ACs results in greater reduction of radial vessel expansion compared with loss of FN or HS, respectively, indicating the importance of VEGF retention to ACs in vessel migration.

FN allele in ACs argues for a dose-dependent regulation of tip-cell migration by FN. In cell culture, a surface-density gradient of FN stimulates haptotaxis and persistent directional migration of microvascular endothelial and CHO cells in a mechanism that involves focal adhesion kinase (FAK) and PI3K (Smith et al., 2006; Rhoads and Guan, 2007). The involvement of FAK would indicate that integrin signalling is important in this process, with PI3K mediating phospho-inositide polarity establishment in the gradient. However, these studies did not investigate the possibility that growth factors such as VEGFA in the culture medium could form a super-imposed gradient through FN interactions. In a follow-up study Liu and colleagues investigated the effect of surface density gradients of FN or VEGFA, as well as a combination of both on the directional migration of endothelial cells (Liu et al., 2007). They report strongest directional migration in combined FN and VEGFA gradients, about twice that seen in VEGF-only gradients and four times greater than that in FN-only gradients. Thus, it is conceivable that the graded production of VEGFA by ACs in combination with the binding to FN could create a cell-surface density gradient of VEGFA that is important for optimal directional migration of endothelial tip cells. Quantitative binding of VEGFA to FN could therefore explain how the FN dose can affect tip cell migration. More FN should establish steeper surface density gradients. It is interesting to note that the slope of the gradients does not directly translate into cell migration speed, but instead influences persistent directionality (Smith et al., 2006; Liu et al., 2007; Rhoads and Guan, 2007). In the retina, the observed reduction in radial vessel migration could very well be caused by less persistent directionality in tip-cell migration.

Crucial VEGF-binding functions in vivo have mostly been attributed to HS, both in zebrafish and mouse models, as well as in tumours (Joyce et al., 2005; Jakobsson et al., 2006; Hawinkels et al., 2008). Blocking the binding of VEGFA to FN by intraocular injection of inhibitory peptides severely affected radial migration, which provides the first in vivo evidence for an important role of VEGFA binding to FN in retinal vascular development. The vascular patterning defects partly resemble the phenotype caused by reduced VEGF gradient formation in $Vegf^{\Delta 20/120}$ mice (Ruhrberg et al., 2002; Gerhardt et al., 2003), supporting the notion of possible gradient defects in FN^{ACko}. However, $Vegf^{\Delta 20/120}$ mice show a greater than 9-12% reduction in radial migration, suggesting that FN^{ACko} mice do retain some ability to generate surface gradients of VEGF on ACs. Our expression analysis and genetic deletion of HS identifies astrocytic HS as additional component that is crucial for radial migration. The magnitude of the radial migration delay (>30%) in compound FN/HS mutants is remarkably similar to $Vegf^{\Delta 20/120}$ mice, suggesting that the loss of both FN and HS disrupts a major part of the astrocytic ability to support VEGFA gradients. Soluble gradients of VEGF121 and VEGF164 in a microfluidic chamber in vitro are equally capable of driving endothelial tip-cell chemotaxis (Barkefors et al., 2008), further supporting the idea that the defects in $Vegf^{\Delta 20/120}$ mice are caused by the absence of a surface density gradient. Surprisingly, the complete deletion of VEGFA from ACs using the same *GFAP Cre* line leads only to a ~10-15% reduction in radial migration at P5 during retinal vascularization (Scott et al., 2010). Moreover, inactivation of the key hypoxia response mechanism by genetic deletion of HIF1α in ACs (Scott et al., 2010), or deletion of the hypoxia-response element in the *Vegfa* promoter (Vinores et al., 2006), has no effect on radial migration. Thus, despite the prominent expression of VEGFA from retinal ACs, and the clear effect of hypoxia on retinal VEGFA expression (West et al., 2005), it appears that other cellular sources can effectively compensate for the loss of astrocytic VEGF expression/regulation. Remarkably, however, endothelial sprouting in these situations still follows the astrocytic template. In the light of our present results, it appears likely that FN and HS on the astrocytic surface would also bind and localize VEGFA on ACs when it is secreted from alternative sources. Thus, we propose that a cell-surface density gradient of VEGF-binding matrix components, such as FN and HS-epitopes, may be even more important than localized VEGFA secretion for guiding sprouting angiogenesis. Intriguingly, a synergistic interaction of HS and FN in growth factor binding and function has recently been described for PDGF-AA in *Xenopus* gastrulation. PDGF-AA binding to FN is enhanced by heparin, and the combined function of FN and endogenous heparan-sulfate mediate directed cell migration of mesendoderm cells towards PDGF-AA (Smith et al., 2009).

In addition to providing a mechanism for retention, FN binding could also play a local role in promoting a co-receptor function for the activation of VEGFR2 (Wijelath et al., 2006), similar to the function of heparan sulfate (Jakobsson et al., 2006; Xu et al., 2011). Integrins and VEGFR2 could engage in signalling complexes and FN can promote complex formation and receptor activation (Hynes, 2009). The cell-binding (integrin) and VEGF-binding domains of FN, when physically linked, promote VEGF-induced endothelial cell functions of FN (Wijelath et al., 2006). In agreement with these findings, Chen and colleagues recently demonstrated that presentation of VEGF in either soluble or matrix-bound form affects the kinetics of VEGFR receptor activation. Matrix-bound VEGF, but not soluble VEGF, induces prolonged activation kinetics of VEGFR2 with altered patterns in tyrosine activation and subsequent downstream enhancement of the p38/MAPK pathway. Notably, the authors bound VEGFA in a collagen matrix, not FN, and thus it remains to be shown whether the events are fully comparable. In collagen matrix, the altered kinetics of activation involved VEGFR2 association with integrin β1 and the redistribution of integrin β1 to focal adhesion complexes. VEGF isoforms that lack matrix-retention domains do not support the association with integrin β1 and the prolonged activation of VEGFR2 (Chen et al., 2010).

In our study, the deletion of astrocytic FN and the disruption of VEGF-FN binding similarly led to reduced VEGFR2 signalling, further supporting the idea that VEGF binding to FN has a function in angiogenesis. VEGF/VEGFR2 signalling mediates endothelial cell functions via activation of signalling pathways such as PI3K, ERK and MAPK. PI3K activity is required for VEGFA-dependent migration of ECs (Gille et al., 2001). Genetic inactivation of the PI3K class 1a catalytic subunit p110a revealed a cell-autonomous function in endothelial tip-cell migration; VEGFA-induced AKT phosphorylation was almost completely abrogated in ECs lacking p110a and migration speed as well as distance was drastically reduced in mice and primary ECs lacking p110a kinase activity (Graupera et al., 2008). Mice carrying only one kinase-dead allele of p110a reveal a 50% reduction in PI3K activity, similar to FN^{ACko} mice, and also a comparable delay in retinal vascularization. These signalling and phenotypic similarities together suggest that the observed PI3K signalling defect is sufficient to explain the reduced radial migration in FN^{ACko} retinas.

How general the observed functions of FN in vivo are for other organs or angiogenesis models remains to be shown. It is, however, likely that instances in which FN-producing cells are also the main source of VEGFA will follow similar principles. This could be relevant for wound healing and for stroma-rich tumours, in which

fibroblasts produce FN and VEGFA, and promote rapid neo-angiogenesis. The observed in vivo effectiveness of the inhibitory peptides against VEGFA binding to FN raises the prospect of using a similar approach to reduce or modulate angiogenic sprouting in tumour angiogenesis or ocular neo-vascularization.

Acknowledgements
We are grateful to Sue Watling, Craig Thrussell, Claire Darnborough and Ayrton Ibbett for excellent animal husbandry and help with tissue collection, and to Nicola O'Reilly and her team at the Peptide Synthesis Laboratory, London Research Institute for peptide synthesis.

Funding
This work was funded by Cancer Research UK, EMBO Young Investigator Program, The Lister Institute of Preventive Medicine, the Leducq Transatlantic Network ARTEMIS (H.G.), DFG and Max-Planck Society. This work was further supported by grants from the National Institutes of Health (RO1 HL079182 to M.S. and E.S.W., PO1-HL66105 and the NIGMS Cell Migration Consortium, GC11451.126452; A. F. Horwitz is the P.I.) and by the Howard Hughes Medical Institute of which R.O.H. is an Investigator. Deposited in PMC for release after 6 months.

Competing interests statement
The authors declare no competing financial interests.

Supplementary material
Supplementary material for this article is available at
http://dev.biologists.org/lookup/suppl/doi:10.1242/dev.071381/-/DC1

References

Abraham, S., Kogata, N., Fassler, R. and Adams, R. H. (2008). Integrin beta1 subunit controls mural cell adhesion, spreading, and blood vessel wall stability. *Circ. Res.* **102**, 562-570.
Bajenaru, M. L., Zhu, Y., Hedrick, N. M., Donahoe, J., Parada, L. F. and Gutmann, D. H. (2002). Astrocyte-specific inactivation of the neurofibromatosis 1 gene (NF1) is insufficient for astrocytoma formation. *Mol. Cell. Biol.* **22**, 5100-5113.
Barkefors, I., Le Jan, S., Jakobsson, L., Hejll, E., Carlson, G., Johansson, H., Jarvius, J., Park, J. W., Li Jeon, N. and Kreuger, J. (2008). Endothelial cell migration in stable gradients of vascular endothelial growth factor A and fibroblast growth factor 2, effects on chemotaxis and chemokinesis. *J. Biol. Chem.* **283**, 13905-13912.
Beech, R. D., Cleary, M. A., Treloar, H. B., Eisch, A. J., Harrist, A. V., Zhong, W., Greer, C. A., Duman, R. S. and Picciotto, M. R. (2004). Nestin promoter/enhancer directs transgene expression to precursors of adult generated periglomerular neurons. *J. Comp. Neurol.* **475**, 128-141.
Chen, T. T., Luque, A., Lee, S., Anderson, S. M., Segura, T. and Iruela-Arispe, M. L. (2010). Anchorage of VEGF to the extracellular matrix conveys differential signaling responses to endothelial cells. *J. Cell Biol.* **188**, 595-609.
Chu, Y., Hughes, S. and Chan-Ling, T. (2001). Differentiation and migration of astrocyte precursor cells and astrocytes in human fetal retina: relevance to optic nerve coloboma. *FASEB J.* **15**, 2013-2015.
Claxton, S., Kostourou, V., Jadeja, S., Chambon, P., Hodivala-Dilke, K. and Fruttiger, M. (2008). Efficient, inducible Cre-recombinase activation in vascular endothelium. *Genesis* **46**, 74-80.
Fontana, L., Chen, Y., Prijatelj, P., Sakai, T., Fassler, R., Sakai, L. Y. and Rifkin, D. B. (2005). Fibronectin is required for integrin alphavbeta6-mediated activation of latent TGF-beta complexes containing LTBP-1. *FASEB J.* **19**, 1798-1808.
Foo, S. S., Turner, C. J., Adams, S., Compagni, A., Aubyn, D., Kogata, N., Lindblom, P., Shani, M., Zicha, D. and Adams, R. H. (2006). Ephrin-B2 controls cell motility and adhesion during blood-vessel-wall assembly. *Cell* **124**, 161-173.
Fruttiger, M. (2002). Development of the mouse retinal vasculature: angiogenesis versus vasculogenesis. *Invest. Ophthalmol. Vis. Sci.* **43**, 522-527.
George, E. L., Georges-Labouesse, E. N., Patel-King, R. S., Rayburn, H. and Hynes, R. O. (1993). Defects in mesoderm, neural tube and vascular development in mouse embryos lacking fibronectin. *Development* **119**, 1079-1091.
George, E. L., Baldwin, H. S. and Hynes, R. O. (1997). Fibronectins are essential for heart and blood vessel morphogenesis but are dispensable for initial specification of precursor cells. *Blood* **90**, 3073-3081.
Gerhardt, H., Golding, M., Fruttiger, M., Ruhrberg, C., Lundkvist, A., Abramsson, A., Jeltsch, M., Mitchell, C., Alitalo, K., Shima, D. et al. (2003). VEGF guides angiogenic sprouting utilizing endothelial tip cell filopodia. *J. Cell Biol.* **161**, 1163-1177.
Gille, H., Kowalski, J., Li, B., LeCouter, J., Moffat, B., Zioncheck, T. F., Pelletier, N. and Ferrara, N. (2001). Analysis of biological effects and signaling properties of Flt-1 (VEGFR-1) and KDR (VEGFR-2). A reassessment using novel receptor-specific vascular endothelial growth factor mutants. *J. Biol. Chem.* **276**, 3222-3230.
Graupera, M., Guillermet-Guibert, J., Foukas, L. C., Phng, L. K., Cain, R. J., Salpekar, A., Pearce, W., Meek, S., Millan, J., Cutillas, P. R. et al. (2008). Angiogenesis selectively requires the p110alpha isoform of PI3K to control endothelial cell migration. *Nature* **453**, 662-666.
Halfter, W., Reinhard, E., Liverani, D., Ortman, R. and Monard, D. (1989). Immunocytochemical localization of glia-derived nexin, laminin and fibronectin on the surface or extracellular matrix of C6 rat glioma cells, astrocytes and fibroblasts. *Eur. J. Neurosci.* **1**, 297-308.
Hawinkels, L. J., Zuidwijk, K., Verspaget, H. W., de Jonge-Muller, E. S., van Duijn, W., Ferreira, V., Fontijn, R. D., David, G., Hommes, D. W., Lamers, C. B. et al. (2008). VEGF release by MMP-9 mediated heparan sulphate cleavage induces colorectal cancer angiogenesis. *Eur. J. Cancer* **44**, 1904-1913.
Hynes, R. O. (2009). The extracellular matrix: not just pretty fibrils. *Science* **326**, 1216-1219.
Inatani, M., Irie, F., Plump, A. S., Tessier-Lavigne, M. and Yamaguchi, Y. (2003). Mammalian brain morphogenesis and midline axon guidance require heparan sulfate. *Science* **302**, 1044-1046.
Ishida, A., Murray, J., Saito, Y., Kanthou, C., Benzakour, O., Shibuya, M. and Wijelath, E. S. (2001). Expression of vascular endothelial growth factor receptors in smooth muscle cells. *J. Cell. Physiol.* **188**, 359-368.
Jakobsson, L., Kreuger, J., Holmborn, K., Lundin, L., Eriksson, I., Kjellen, L. and Claesson-Welsh, L. (2006). Heparan sulfate in trans potentiates VEGFR-mediated angiogenesis. *Dev. Cell* **10**, 625-634.
Jiang, B., Liou, G. I., Behzadian, M. A. and Caldwell, R. B. (1994). Astrocytes modulate retinal vasculogenesis: effects on fibronectin expression. *J. Cell Sci.* **107**, 2499-2508.
Joyce, J. A., Freeman, C., Meyer-Morse, N., Parish, C. R. and Hanahan, D. (2005). A functional heparan sulfate mimetic implicates both heparanase and heparan sulfate in tumor angiogenesis and invasion in a mouse model of multistage cancer. *Oncogene* **24**, 4037-4051.
Kisanuki, Y. Y., Hammer, R. E., Miyazaki, J., Williams, S. C., Richardson, J. A. and Yanagisawa, M. (2001). Tie2-Cre transgenic mice: a new model for endothelial cell-lineage analysis in vivo. *Dev. Biol.* **230**, 230-242.
Leiss, M., Beckmann, K., Giros, A., Costell, M. and Fassler, R. (2008). The role of integrin binding sites in fibronectin matrix assembly in vivo. *Curr. Opin. Cell Biol.* **20**, 502-507.
Liesi, P., Kirkwood, T. and Vaheri, A. (1986). Fibronectin in expressed by astrocytes cultured from embryonic and postnatal rat brain. *Exp. Cell Res.* **163**, 175-185.
Liu, L., Ratner, B. D., Sage, E. H. and Jiang, S. (2007). Endothelial cell migration on surface-density gradients of fibronectin, VEGF, or both proteins. *Langmuir* **23**, 11168-11173.
Petersen, P. H., Zou, K., Hwang, J. K., Jan, Y. N. and Zhong, W. (2002). Progenitor cell maintenance requires numb and numblike during mouse neurogenesis. *Nature* **419**, 929-934.
Rhoads, D. S. and Guan, J. L. (2007). Analysis of directional cell migration on defined FN gradients: role of intracellular signaling molecules. *Exp. Cell Res.* **313**, 3859-3867.
Risau, W. and Lemmon, V. (1988). Changes in the vascular extracellular matrix during embryonic vasculogenesis and angiogenesis. *Dev. Biol.* **125**, 441-450.
Ruhrberg, C., Gerhardt, H., Golding, M., Watson, R., Ioannidou, S., Fujisawa, H., Betsholtz, C. and Shima, D. T. (2002). Spatially restricted patterning cues provided by heparin-binding VEGF-A control blood vessel branching morphogenesis. *Genes Dev.* **16**, 2684-2698.
Sakai, T., Johnson, K. J., Murozono, M., Sakai, K., Magnuson, M. A., Wieloch, T., Cronberg, T., Isshiki, A., Erickson, H. P. and Fassler, R. (2001). Plasma fibronectin supports neuronal survival and reduces brain injury following transient focal cerebral ischemia but is not essential for skin-wound healing and hemostasis. *Nat. Med.* **7**, 324-330.
Scott, A., Powner, M. B., Gandhi, P., Clarkin, C., Gutmann, D. H., Johnson, R. S., Ferrara, N. and Fruttiger, M. (2010). Astrocyte-derived vascular endothelial growth factor stabilizes vessels in the developing retinal vasculature. *PLoS ONE* **5**, e11863.
Smith, E. M., Mitsi, M., Nugent, M. A. and Symes, K. (2009). PDGF-A interactions with fibronectin reveal a critical role for heparan sulfate in directed cell migration during *Xenopus* gastrulation. *Proc. Natl. Acad. Sci. USA* **106**, 21683-21688.
Smith, J. T., Elkin, J. T. and Reichert, W. M. (2006). Directed cell migration on fibronectin gradients: effect of gradient slope. *Exp. Cell Res.* **312**, 2424-2432.
Stone, J., Itin, A., Alon, T., Peer, J., Gnessin, H., Chan-Ling, T. and Keshet, E. (1995). Development of retinal vasculature is mediated by hypoxia-induced vascular endothelial growtn factor (VEGF) expression by neuroglia. *J. Neurosci.* **15**, 4738-4747.
Takahashi, S., Leiss, M., Moser, M., Ohashi, T., Kitao, T., Heckmann, D., Pfeifer, A., Kessler, H., Takagi, J., Erickson, H. P. et al. (2007). The RGD motif

in fibronectin is essential for development but dispensable for fibril assembly. *J. Cell Biol.* **178**, 167-178.

Thompson, S. M., Fernig, D. G., Jesudason, E. C., Losty, P. D., van de Westerlo, E. M., van Kuppevelt, T. H. and Turnbull, J. E. (2009). Heparan sulfate phage display antibodies identify distinct epitopes with complex binding characteristics: insights into protein binding specificities. *J. Biol. Chem.* **284**, 35621-35631.

Uemura, A., Kusuhara, S., Wiegand, S. J., Yu, R. T. and Nishikawa, S. (2006). Tlx acts as a proangiogenic switch by regulating extracellular assembly of fibronectin matrices in retinal astrocytes. *J. Clin. Invest.* **116**, 369-377.

van der Flier, A., Badu-Nkansah, K., Whittaker, C. A., Crowley, D., Bronson, R. T., Lacy-Hulbert, A. and Hynes, R. O. (2010). Endothelial alpha5 and alphav integrins cooperate in remodeling of the vasculature during development. *Development* **137**, 2439-2449.

Vinores, S. A., Xiao, W. H., Aslam, S., Shen, J., Oshima, Y., Nambu, H., Liu, H., Carmeliet, P. and Campochiaro, P. A. (2006). Implication of the hypoxia response element of the Vegf promoter in mouse models of retinal and choroidal neovascularization, but not retinal vascular development. *J. Cell. Physiol.* **206**, 749-758.

West, H., Richardson, W. D. and Fruttiger, M. (2005). Stabilization of the retinal vascular network by reciprocal feedback between blood vessels and astrocytes. *Development* **132**, 1855-1862.

Wijelath, E. S., Murray, J., Rahman, S., Patel, Y., Ishida, A., Strand, K., Aziz, S., Cardona, C., Hammond, W. P., Savidge, G. F. et al. (2002). Novel vascular endothelial growth factor binding domains of fibronectin enhance vascular endothelial growth factor biological activity. *Circ. Res.* **91**, 25-31.

Wijelath, E. S., Rahman, S., Namekata, M., Murray, J., Nishimura, T., Mostafavi-Pour, Z., Patel, Y., Suda, Y., Humphries, M. J. and Sobel, M. (2006). Heparin-II domain of fibronectin is a vascular endothelial growth factor-binding domain: enhancement of VEGF biological activity by a singular growth factor/matrix protein synergism. *Circ. Res.* **99**, 853-860.

Xu, D., Fuster, M. M., Lawrence, R. and Esko, J. D. (2011). Heparan sulfate regulates VEGF165- and VEGF121-mediated vascular hyperpermeability. *J. Biol. Chem.* **286**, 737-745.

Yang, J. T., Rayburn, H. and Hynes, R. O. (1993). Embryonic mesodermal defects in alpha5 integrin-deficient mice. *Development* **119**, 1093-1105.

Yang, J. T., Bader, B. L., Kreidberg, J. A., Ullman-Cullere, M., Trevithick, J. E. and Hynes, R. O. (1999). Overlapping and independent functions of fibronectin receptor integrins in early mesodermal development. *Dev. Biol.* **215**, 264-277.